Prediction of adsorption isotherms from breakthrough curves

Poursaeidesfahani, Ali; Andres-Garcia, Eduardo; de Lange, Martijn; Torres-Knoop, Ariana; Rigutto, Marcello; Nair, Nitish; Kapteijn, Freek; Gascon, Jorge; Dubbeldam, David; Vlugt, Thijs J.H.

DOI
10.1016/j.micromeso.2018.10.037

Publication date
2019

Document Version
Accepted author manuscript

Published in
Microporous and Mesoporous Materials

Prediction of adsorption isotherms from breakthrough curves

Ali Poursaeidesfahani[a], Eduardo Andres-Garcia[b], Martijn de Lange[a], Ariana Torres-Knoop[c], Marcello Rigutto[d], Nitish Nair[e], Freek Kapteijn[b], Jorge Gascon[f], David Dubbeldam[c], Thijs J.H. Vlugt[a,]

[a] *Engineering Thermodynamics, Process & Energy Department, Faculty of Mechanical, Maritime and Materials Engineering, Delft University of Technology, Leeghwaterstraat 39, 2628CB, Delft, The Netherlands*

[b] *Chemical Engineering Department, Catalysis Engineering, Faculty of Applied Sciences, Delft University of Technology, Julianalaan 136, 2628 BL Delft, The Netherlands*

[c] *Van't Hoff Institute for Molecular Sciences, University of Amsterdam, Science Park 904, 1098XH Amsterdam, The Netherlands*

[d] *Shell Global Solutions International, PO Box 38000, 1030BN Amsterdam, The Netherlands*

[e] *Shell India Markets Private Limited, Kundanahalli Main Road, Bangalore 560048, Karnataka, India*

[f] *King Abdullah University of Science and Technology, KAUST Catalysis Center, Advanced Catalytic Materials, Thuwal 23955, Saudi Arabia*

Abstract

A mathematical model is used to predict adsorption isotherms from experimentally measured breakthrough curves. Using this approach, by performing only breakthrough experiments for a mixture of two (or more) components, one can obtain pure component adsorption isotherms up to the pressure of the experiment. As a case study, the adsorption of an equimolar mixture of CO_2 and CH_4 in zeolite ITQ-29 is investigated. Pure component linear adsorption isotherms for CO_2 and CH_4 are predicted by fitting the theoretical breakthrough curves to the experimental ones. Henry coefficients obtained from our approach are in excellent agreement with those measured experimentally. A similar procedure is applied to predict the complete Langmuir adsorption isotherm from breakthrough curves at high pressures. The resulting adsorption isotherms are in very good agreement with those measured experimentally. In our model for transient adsorption, mass transfer from the gas phase to the adsorbed phase is considered using the Linear Driving Force model and dispersion of the gas phase in the packed bed is taken into account. IAST is used to compute the equilibrium loadings for a mixture of gases. The influence of the dispersion coefficient and the effective mass transfer coefficient on the shape of breakthrough curves is investigated and discussed. Rough estimations of these values are sufficient to predict adsorption isotherms from breakthrough curves.

Keywords: Breakthrough curve, Adsorption isotherm, Dispersion, Mass transfer

Email address: t.j.h.vlugt@tudelft.nl (Thijs J.H. Vlugt)

1. Introduction

Separation processes based on adsorption are becoming increasingly popular [1, 2, 3]. This is mainly due to the recent sharp growth in the number of potential adsorbents [4]. Traditionally, the best adsorbent for a process is selected by conducting several experiments. Experimentally measured adsorption isotherms and breakthrough curves are conventionally used to design new adsorption based separation processes. Adsorption isotherms are the outcome of static adsorption experiments where the adsorbate and adsorbent are kept in contact for a long time until equilibrium is reached [5]. The equilibrium loadings measured at constant temperature and various pressures are used to construct adsorption isotherms. In dynamic adsorption experiments, a fluid phase containing the adsorbate flows over a fixed bed of adsorbent. Breakthrough curves show the concentration of an adsorbate in the fluid phase at the outlet of the adsorption column as a function of time[6]. This experimental procedure, from preparing a sample to analysing the results, can be very time consuming and expensive. Hence, it is not feasible to experimentally screen a large number of potential adsorbents for each separation process. One of the most efficient ways to select an appropriate adsorbent and find the optimal operating conditions for an adsorption based separation is the modeling of the transient adsorption process [7, 8]. In the most detailed mathematical model, a large set of Partial Differential Equations (PDEs) including mass, energy and momentum balances has to be solved for the fixed bed [9]. Considering all these details makes calculations time consuming. Therefore, simplifying assumptions are usually applied to facilitate the computational process without losing the predictive capability of mathematical models. During the last decades, several models with various simplifications have been proposed to reproduce and predict the experimental breakthrough curves for different systems[10, 8, 11, 12, 9, 13, 14]. Breakthrough curves estimated by many of these models are in good agreement with the experimental breakthrough curves [7, 13, 14]. However, the application of an efficient model for simulating transient adsorption processes is not limited to the prediction of the breakthrough curves.

In this paper, we use a mathematical model for other purposes such as estimating the adsorption isotherms from breakthrough curves and investigating the effects of mass transfer and gas phase dispersion on the shape of breakthrough curves. Adsorption isotherms and breakthrough curves are essentially the static and dynamic outcomes of adsorption processes. Therefore, in principle, a mathematical model considering all relevant mass and energy transport phenomena could be used to estimate an adsorption isotherm from the corresponding breakthrough curve. Obtaining an experimental adsorption isotherm is, in general, more time consuming (and involves more experiments) compared to obtaining a breakthrough curve for the same system. Consequently, it would be beneficial if one can obtain both the breakthrough curve and the adsorption isotherm only by performing breakthrough experiments. The idea of predicting adsorption isotherms from experimentally measured breakthrough curves has attracted many researchers for decades [15, 16, 17, 18, 19]. One of the mostly used approaches to determine adoption isotherms from the breakthrough curves is based on the classical equilibrium theory [18, 19]. Many excellent papers have been published on the application of this theory[20, 21, 22, 23]. This theory neglects all

the kinetic effects and just considers convection and equilibrium distribution between the phases which is defined by thermodynamics. The nice feature of this approach is that, by the exclusion of kinetics,the dynamic measurements (breakthrough curves) and thermodynamic predictions (adsorption isotherms) are directly related[24, 25]. This is also the main limitation of the approach which prohibits its application for the cases with significant kinetic effects causing band broadening. For a system with N components by identifying $N-1$ intermediate plateau concentrations and N retention times of shock fronts one would be able to compute the equilibrium loading for certain conditions[15, 16]. The retention times are usually calculated by integrating the breakthrough curves. If the breakthrough curves are significantly eroded due to kinetic effects it is difficult to calculate the retention times and estimate the intermediate plateau concentrations. The other disadvantage of the equilibrium theory is that one can only obtain a single point per breakthrough experiment on the mixture adsorption isotherm for each component at certain conditions. Therefore, one needs to perform several experiments to obtain the entire adsorption isotherm. In this paper, we introduce an approach to obtain the complete pure adsorption isotherms for all the components in the system with limited number of breakthrough experiments. Together with IAST it can be used to compute the equilibrium loading for each component in the mixture at any composition and condition. We used our approach to obtain adsorption isotherms from significantly eroded breakthrough curves when equilibrium theory is not applicable.
This paper is organized as follows. Experimental details are provided in section 2. In section 3, the mathematical model used for modeling the transient adsorption process and its main assumptions are summarized. Estimation of adsorption isotherms from experimentally measured breakthrough curves is described as an optimization problem. In section 4, the effects of mass transfer resistance and dispersion in the gas phase on the shape of breakthrough curves are investigated. The Henry coefficients obtained from our approach, using experimentally measured breakthrough curves at pressure of 2 bar, are compared with the experimental values. The same procedure is applied to predict the complete adsorption isotherm from breakthrough curves at higher pressures. Our findings are summarized in section 5.

2. Experiments

2.1. Adsorbent

Pure-silica (Al-free) ITQ-29 is a hydrophobic 8MR zeolite, able to sieve small organic molecules with a high precision, even in the presence of water[26]. The complete absence of acidity allows separations even in the presence of olefins. This is not possible with Al-containing zeolites due to oligomerization and pore blocking[27]. This pure-silica zeolite, analysed with SEM (Scanning Electron Microscopy), presents a homogeneous distribution of cubic particles of 2.00 μm (see Fig. 1).

2.2. Pure Component Adsorption Isotherm Measurement

The adsorbent (ITQ-29 powder) is weighed and outgassed overnight under vacuum condition at 473 K. Gas adsorption is performed by the volumetric method, using a high-pressure

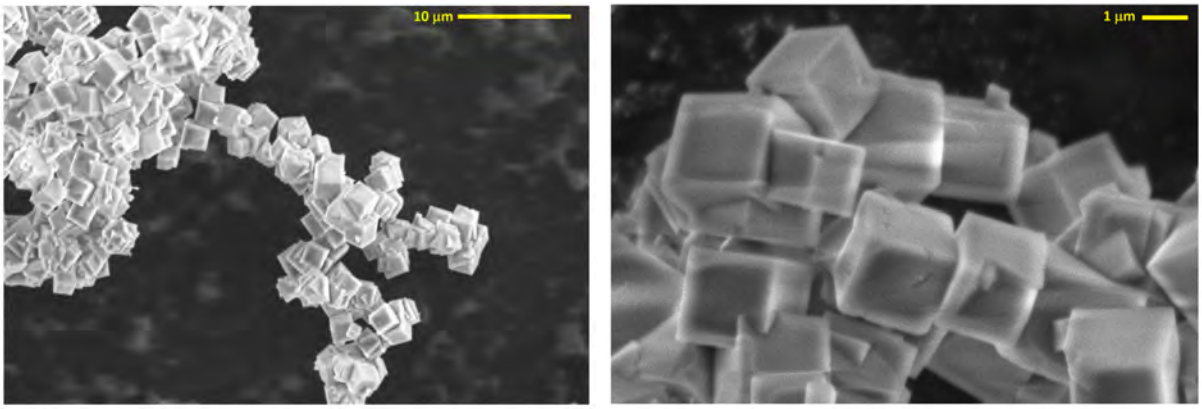

Figure 1: SEM images of ITQ-29 zeolite used in this study.

gas adsorption system BELSORP-HP (BEL Japan, INC). The adsorption isotherms for CO_2 and CH_4 are obtained by an equilibration time of 1200 s between different pressure steps. All experiments are performed at 298 K.

2.3. Breakthrough Experiments

Breakthrough experiments are carried out to study the performance of a packed bed of ITQ-29 pellets for separating CO_2/CH_4 mixtures. 220 mg of ITQ-29 self-sustained pelletized (pellet density 1016 kg m^{-3}, particles size between 500 and 720 μm, pelletizing pressure 5 ton cm^{-2}) are placed inside the column. To control the composition of the gas mixture, separate flow controllers are used to adjust the flow rate of different components upstream of the mixing section. In this mixing section, CO_2 and CH_4 with equal flow rates of 5 ml min^{-1} are mixed with hydrogen. Hydrogen, with the flow rate of 1 ml min^{-1}, is used as a non-adsorbing tracer. The total pressure of the gas mixture is controlled at the outlet of the adsorption column. The pressure of the system is maintained at 2 bar. At these conditions, the pressure drop across the column is negligible. An adsorption column with an inner diameter of 0.4 cm and a length of 7 cm is placed inside an oven to ensure isothermal condition throughout the experiment. Before starting the experiments the column is filled with He at the pressure of the experiment and 298 K. The temperature of the column is kept at 298 K throughout the experiments. A Quadrupole Mass Spectrometer (QMS200-PRISMATM with GSD 300 O/T, using Electron Ionization) is used to analyse the composition of the gas mixture breaking through the column. At the column exit a flow of 100 ml min^{-1} He is added to avoid gas stand still in case of adsorption of both components, and to allow calculation of component flow rates exiting the column based on MS analysis[6]. More details regarding the experimental setup can be found elsewhere [28, 6].

3. Mathematical Model

Our mathematical model is mainly formed by the transient material balance of the fluid phase and the adsorbed phase and the momentum balance (Ergun equation) [29], neglecting heat transfer effects [30]. The material balance of the fluid phase includes the spatial

(axial) and temporal variations of concentrations of all components in the fluid phase. The adsorbed phase material balance describes the variations in the loading of each component along the column. The fluid and adsorbed phase material balances are coupled by the mass transfer between the two phases.
The migration of adsorbate molecules from the gas phase into the adsorbent and vice versa are described by Linear Driving Force model (LDF-model)[31, 32, 33]. Sircar and Hufton compared LDF-model with the more rigorous Fickian diffusion [34]. These authors showed that all details regarding the intra-pore diffusion are lost, when modeling breakthrough curves using Fickian diffusion. Therefore, the LDF-model is a sufficient and efficient approximation for computing breakthrough curves [34]. The LDF-model is often formulated as follows:

$$\frac{\partial \bar{q}_{i,\mathrm{ads}}}{\partial t} = k_{L,i}\left(q_{i,\mathrm{eq}} - \bar{q}_{i,\mathrm{ads}}\right) \tag{1}$$

Here, $\bar{q}_{i,\mathrm{ads}}$ is the average loading in the adsorbent as a function of time, $k_{L,i}$ is the effective mass transfer coefficient of component i (s^{-1}), and $q_{i,\mathrm{eq}}$ is the equilibrium loading of component i for given gas phase conditions. By definition, when the adsorbed phase is in equilibrium with the gas phase, there is no net mass transfer between the phases. The equilibrium loadings ($q_{i,\mathrm{eq}}$) for components present in the mixture are computed using the Ideal Adsorption Solution Theory (IAST) [35, 36, 37]. IAST makes use of pure component isotherms to estimate the equilibrium loading of each component in a mixture. To facilitate the application of IAST, based on the shape of the experimentally measured pure component isotherms, a functional form (e.g. Langmuir, Langmuir-Freundlich) is fitted to each pure component isotherm data. In this way, it is trivial to obtain an analytical expression for the spreading pressure of each component. Spreading pressures are then used to compute the equilibrium loading of each component in the gas mixture. Note that IAST fails to provide accurate estimation of equilibrium loadings when there is a strong segregation in the preferable adsorption sites for different components[38, 39]. This is not the case for the system under study. For more information about IAST, readers are referred to the original publications [35, 36, 37, 40].
Assuming ideal gas behaviour for the gas phase, the material balance for each component in the gas phase is described by [33, 41]

$$\frac{1}{RT}\frac{\partial p_i}{\partial t} = -\frac{1}{RT}\frac{\partial\left(u p_i\right)}{\partial \mathrm{z}} + \frac{1}{RT} D_i \frac{\partial^2 p_i}{\partial \mathrm{z}^2} - \left(\frac{1-\varepsilon}{\varepsilon}\right)\rho_{\mathrm{P}} k_{L,i}(q_{i,\mathrm{eq}} - \bar{q}_{i,\mathrm{ads}}) \tag{2}$$

where p_i is the partial pressure of component i in the gas phase, u is the interstitial velocity of the gas phase, D_i is the axial dispersion coefficient for component i, and ε is the void fraction of the column packing. The first term on the right hand side of Eq. 2 accounts for the effect of convective mass transport. The second term on the right shows the effect of axial dispersion on the overall mass balance of the gas phase and the last term takes in to account the influence of mass transfer between the adsorbed phase and the gas phase. Radial gradients are assumed absent. Velocity profiles in packed beds due to radial packing gradients can be neglected for sufficiently small particles compared to the column diameter.

One can rewrite Eq. 2 using dimensionless parameters:

$$\frac{1}{RT}\frac{\partial p_i}{\partial \tau} = -\frac{1}{RT}\frac{\partial\left(v p_i\right)}{\partial \zeta} + \frac{1}{RTPe_i}\frac{\partial^2 p_i}{\partial \zeta^2} - \left(\frac{1-\varepsilon}{\varepsilon}\right)\rho_{\mathrm{P}} k'_{L,i}(q_{i,\mathrm{eq}} - \bar{q}_{i,\mathrm{ads}}) \tag{3}$$

where

$$\begin{aligned}
\tau &= t\frac{u_{\mathrm{in}}}{L} \\
\zeta &= \frac{z}{L} \\
v &= \frac{u}{u_{\mathrm{in}}} \\
\frac{1}{Pe_i} &= D'_i = \frac{D_i}{L u_{\mathrm{in}}} \\
k'_L &= k_L\frac{L}{u_{\mathrm{in}}}
\end{aligned}$$

Here, L is the length of the column, u_{in} is the interstitial velocity at the inlet of the column, and Pe is the Péclet number. In literature, the Péclet number is commonly used to refer to the dimensionless dispersion coefficient [42]. It is important to note that the characteristic length of particle and not the length of the column is sometimes used in the definition of the Péclet number. The pressure drop along the fixed bed follows from the momentum balance and can be estimated using the Ergun equation [29]. It is assumed that the pressure gradient (if any) is constant and not affected by the adsorption process. As a result, the pressure varies linearly along the length of the column and remains constant with time. Therefore, the overall mass balance equation can be summarized as:

$$\begin{aligned}
&\frac{\partial p_{\mathrm{t}}}{\partial \tau} = 0, \frac{\partial p_{\mathrm{t}}}{\partial \zeta} = \text{constant} \\
&\frac{1}{RT}\left(p_{\mathrm{t}}\frac{\partial v}{\partial \zeta} + v\frac{\partial p_{\mathrm{t}}}{\partial \zeta}\right) = -\sum_{i=1}^{N}\left[\left(\frac{1-\varepsilon}{\varepsilon}\right)\rho_{\mathrm{P}} k'_L(q_{i,\mathrm{eq}} - \bar{q}_{i,\mathrm{ads}}) - \frac{1}{RTPe}\frac{\partial^2 p_i}{\partial \zeta^2}\right]
\end{aligned} \tag{4}$$

In this equation, p_{t} is the total pressure of the gas phase and N is the number of components in the gas phase. Eq. 4 can be rearranged to obtain an expression for the term $\frac{\partial v}{\partial z}$

$$\frac{\partial v}{\partial \zeta} = \frac{1}{p_{\mathrm{t}}}\left[-RT\left(\sum_{i=1}^{N}\left[\left(\frac{1-\varepsilon}{\varepsilon}\right)\rho_{\mathrm{P}} k'_L(q_{i,\mathrm{eq}} - \bar{q}_{i,\mathrm{ads}}) - \frac{1}{RTPe}\frac{\partial^2 p_i}{\partial \zeta^2}\right]\right) - v\frac{\partial p_{\mathrm{t}}}{\partial \zeta}\right] \tag{5}$$

The mathematical model consists of a system of Partial Differential Equations subject to following boundary and initial conditions:

Initial conditions:

$$\begin{aligned}
p_i(0,\zeta) &= 0 \\
p_{He}(0,\zeta) &= p_t(0,\zeta) \\
\bar{q}_{i,\mathrm{ads}}(0,\zeta) &= 0
\end{aligned}$$

Boundary conditions:

$$v(\tau, 0) = 1$$
$$p_i(\tau, 0) = p_{i,\text{in}}$$
$$p_t(\tau, \zeta) = p_t(0, \zeta)$$
$$\frac{\partial p_i}{\partial \zeta}(\tau, 0) = 0$$

The system of equations is discretized in time and space using finite difference approximations and solved step wise in time. Spatial partial derivatives are approximated by second order upwind method. In each time step, a system of $2N \times n$ equations is solved, where N is the number of components and n is the number of grid points in the axial directions. The numerical method of lines with the implicit trapezoidal rule is used to perform integration in time[43]. The values for partial pressures and loadings of each component in the next time step are first approximated using the first order forward approximation. These values are used in an iterative scheme using the implicit trapezoidal rule. Our model is implemented in MATLAB and has been validated by comparing the simulation results with other existing breakthrough models developed independently by other groups[44, 45]. The code can handle the adsorption of multi-component mixtures as well as pure gases with various functional forms for the adsorption isotherm. In summary, the following assumptions are made: (1) the gas phase behaves as an ideal gas; (2) the system is isothermal (this assumption is valid when the heat of adsorption is not too high. If required the none isothermal case can be modeled by including an energy balance); (3) radial variations in concentration are negligible compared to axial variations in the bed; (4) mass transfer between the gas phase and the adsorbed phase can be described by the effective LDF-model; (5) the adsorbed phase is homogeneous; (6) IAST is applicable.

3.1. Estimation of the adsorption properties

It is assumed that the adsorption isotherms for CO_2 and CH_4 in zeolite ITQ-29 are unknown. Instead, the experimental breakthrough curves for the equimolar mixture of CO_2 and CH_4 passing through a fixed bed of zeolite ITQ-29, at total pressures of 2-16 bar and temperature of 298 K, are available. The mathematical model is used to estimate the adsorption isotherms by fitting the theoretical breakthrough curves to the experimental ones. The Mean Sum of Squared of Residuals (MSSR) is the natural objective function for this optimization problem. The residual at each data point is defined as the difference between the experimental and theoretical concentration of component i. The objective function is given by

$$MSSR = \frac{\sum_{j=0}^{n} \left(C_{i,j,\text{out,model}} - C_{i,j,\text{out,exp}}\right)^2}{n - n_\text{P}} \tag{6}$$

where n is the number of data points available from the breakthrough experiment, n_P is the number of estimated parameters, and $C_{i,j,\text{out,model}}$ is the concentration of component i at the outlet of the column predicted by model. Input parameters for the mathematical model include specifications of the adsorption column (length and inner diameter), density and

amount of adsorbent placed inside the adsorption column, gas phase composition and flow rate, pressures at the inlet and outlet of the adsorption column, mass transfer coefficient, and the Péclet number. The main output of the mathematical model are absolute adsorption isotherms for each of the components up to the pressure of the experiment.

Breakthrough curves are generated by collecting the last points of the instantaneous spatial concentration profiles in the gas phase throughout the experiment (or calculation). As the adsorbing gases proceed through the column, the partial pressures at different points of the column change differently from zero to partial pressures at the inlet and even higher (for the less adsorbing component when it is displaced by a more adsorbing component). Therefore, during the breakthrough experiment each point of the column experiences the whole pressure range of the adsorption isotherm from zero to the inlet partial pressure (or even higher). For the case of mixture, the equilibrium loading of each component depends on the partial pressures of all components. By fitting to the breakthrough curves and using the adsorption isotherms as variables, information from the breakthrough curves are extracted and used more efficiently and the adsorption isotherms of all components can be estimated more accurately.

4. Results

4.1. Mass transfer coefficient and Péclet number

The estimation of the effective mass transfer coefficient and the Péclet number requires detailed information regarding the properties of the system and it is not always straightforward[46]. This information is not always available and even if it is, experimental correlations and can only provide an estimation of the effective mass transfer coefficient and the Péclet number. Therefore, it is advantageous to investigate the influence of these parameters on the theoretical breakthrough curves and eventually the adsorption isotherms fitted by the model. To investigate the effect of k'_L and Pe on the shape of the theoretical breakthrough curves, the theoretical breakthrough curves corresponding to different mass transfer coefficients and the Péclet numbers are compared in Fig. 2. In some studies, it is assumed that the value of effective mass transfer coefficient is identical for all components. This assumption does not necessarily hold for components with very different sizes, specially when micropore diffusion is important. Therefore, in this section, separate mass transfer coefficients but identical Péclet numbers are considered for different components. In Fig. 2, $t = 0$ is the breakthrough time of hydrogen (defined as the time at which hydrogen partial pressure at the outlet of the column reaches 10% of its inlet partial pressure). He content is excluded while calculating the mole fractions.

In both cases (Figs. 2a and 2b), increasing the mass transfer coefficient results in steeper breakthrough curve, while delaying the breakthrough time. Due to the increase in the mass transfer rate, larger mass transfer coefficients result in steeper concentration profile of the adsorbing gases along the column. Therefore, the first traces of both gases are observed later for cases where the mass transfer coefficient is higher, and the mole fractions at the outlet of the column increase more rapidly compared to cases with a lower mass transfer coefficient (see Fig. 2). Comparing Figs. 2a and 2b, two important points are observed: (1)

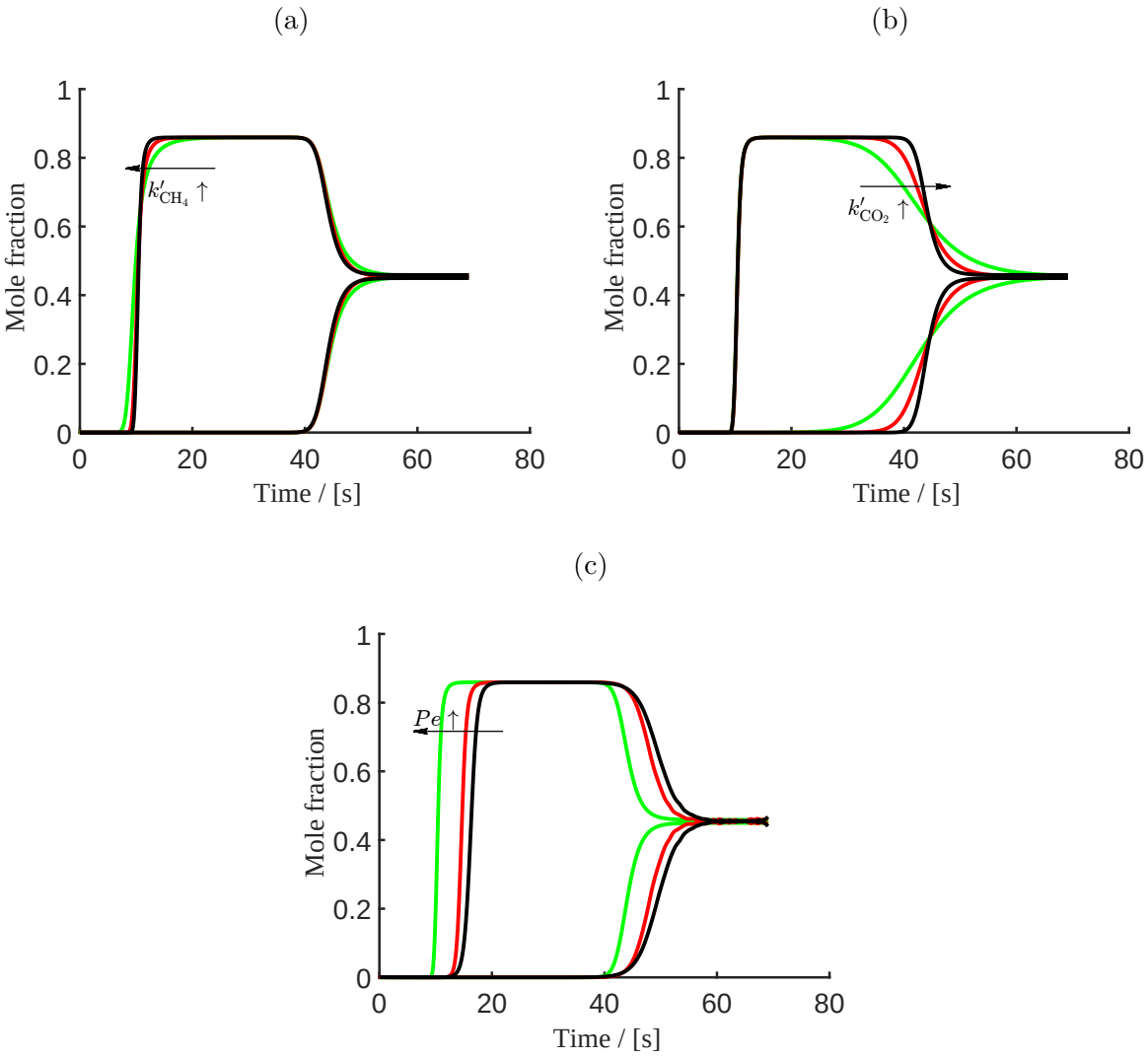

Figure 2: Theoretical breakthrough curves obtained for different sets of mass transfer coefficient and Péclet number (a) $Pe = \infty$, $k'_{CO_2} = 15$ and $k'_{CH_4} = 15$ black, 7 red, 3 green (b) $Pe = \infty$, $k'_{CH_4} = 15$ and $k'_{CO_2} = 15$ black, 7 red, 3 green (c) $k'_{CO_2} = 15$, $k'_{CH_4} = 15$ and $Pe = 250$ black, 500 red, ∞ green. An equimolar mixture of CO_2 and CH_4 is adsorbed by ITQ-29 zeolite at 2 bar and 298 K. Note: the experimentally measured Henry coefficients are used in these breakthrough calculations ($K^{exp}_{H,CO_2} = 1.2$ [mol kg^{-1} bar^{-1}], $K^{exp}_{H,CH_4} = 0.3$ [mol kg^{-1} bar^{-1}]).

preferentially adsorbed component has a more gradual (less steep) breakthrough curve even for the cases that identical mass transfer coefficients are assumed for the two components; (2) mass transfer coefficient of the component which is preferentially adsorbed has a more pronounced influence on the shape of the breakthrough curves. There are two parameters that can influence the steepness of breakthrough curves: (1) the average velocity of the Mass Transfer Zone (MTZ) and (2) the steepness of the concentration profile along the column. The average velocity of the Mass Transfer Zone V_{MTZ} is proportional to $\frac{\dot{Q}_{i,\mathrm{in}}}{a \times q_{i,\mathrm{eq}}^{\mathrm{in}} + b}$, where $\dot{Q}_{i,\mathrm{in}}$ is the volume flow rate of component i and $q_{i,\mathrm{eq}}^{\mathrm{in}}$ is the equilibrium loading of component i at the inlet conditions. a and b are constants defined by the void fraction, density of the adsorbent and conditions of the experiment. Higher values of V_{MTZ} can be interpreted as shorter time difference between the breakthrough time and the time that the concentration at the outlet reaches its plateau. Therefore, higher values of V_{MTZ} leads to steeper breakthrough curve. For the limiting case when $q_{i,\mathrm{eq}}^{\mathrm{in}} = 0$, breakthrough curve will be the steepest. As the two components have identical flow rates and same inlet conditions (50-50 mixture), the component with the higher value of $q_{i,\mathrm{eq}}^{\mathrm{in}}$ (higher Henry coefficient) is expected to have the lower values of V_{MTZ} and less steep breakthrough curve (Figs. 2a and 2b). As $q_{i,\mathrm{eq}}^{\mathrm{in}}$ increases, the influence of the second parameter, the steepness of the concentration profile, becomes more important. The steepness of the concentration profile is reduced by decreasing the mass transfer coefficient (Figs. 2a and 2b). It should be mentioned that unlike the thermodynamic properties (e.g. adsorption isotherm) kinetic properties (e.g. mass transfer coefficient) strongly depend on the crystal size and other physical properties of the adsorbent. Therefore, it is important to estimate the kinetic parameters for each situation. Simulated breakthrough curves for different values of Péclet number are shown in Fig. 2c. Increasing the value of Péclet number (lowering the dispersion coefficient) shifts both breakthrough curves to the left. That is mainly due to displacement of $t = 0$ (the breakthrough time of hydrogen). Higher dispersion coefficient makes the concentration profile less steep and more gradual. The concentration gradient along the axis of the column is the driving force for the axial dispersion. Consequently, axial dispersion smoothes the breakthrough curves and makes the changes in mole fraction (with respect to time and space) more gradual. In general, a larger axial dispersion coefficient (lower value for Pe) results in larger deviations from plug flow and more gradual changes in concentrations. This can have a considerable effect on the breakthrough time of none-adsorbing component. Therefore, for higher values of dispersion coefficient, hydrogen reaches the outlet of the column faster which shifts the $t = 0$ to the left and results in longer breakthrough times for the adsorbing components. The analysis above is in agreement with general theory on this topic[47, 48, 49]. Assuming that the film resistance and macropore diffusion are the limiting steps for the mass transfer between the two phases, the dimensionless effective mass transfer coefficient is roughly estimated by ($k'_L \approx [10^0 - 10^1]$). Empirical correlations are used to estimate the effective mass transfer coefficients ($k_{L,i}$). These correlations are discussed in the Supporting Information. As suggested in Ref.42, it is assumed that the molecular diffusivity (D_M) is of the order of magnitude 10^{-7} m^2/s [50].

4.2. Estimation of Henry coefficients

Experiments are performed at total pressure of 2 bar. To compute the theoretical breakthrough curves, the adsorption isotherms of pure components are required only up to the pressure of 2 bar. At this pressure, the loading is so low that it can be safely assumed that the enthalpy of adsorption is independent of loading. In this region and for this system, the loading is a linear function of external pressure and normally described by the Henry coefficient:

$$q_{i,\mathrm{eq}} = K_{H,i} p \tag{7}$$

where p_i is the partial pressure of the component i and $K_{H,i}$ is the Henry coefficient. The pure component adsorption isotherms are measured experimentally and it has been confirmed that the loading is a linear function of external pressure (see SI). Experimentally measured adsorption isotherms for CO_2 and CH_4 in ITQ-29 at 298 K and their corresponding Henry coefficients are presented in SI. It is important to note that experimental breakthrough curves cannot provide any information regarding the pure components equilibrium loadings at pressures larger than the pressure of the experiment. By fitting the theoretical breakthrough curves to the experimental ones, the adsorption isotherms can only be estimated up to the pressure of the experiment. Since, in this region, the pure component equilibrium loadings of both components (CO_2 and CH_4) are linear functions of pressure, the Henry adsorption coefficients and mass transfer coefficients of the two components are the parameters that are estimated by the model. To investigate the importance of initial values, the optimization process is started with several initial values for the dimensionless mass transfer coefficients of two components within the range of (1-15) and Henry coefficients for CO_2 in range of (0.5-1.5 [mol kg^{-1} bar^{-1}]) and for CH_4 in range of (0.1-0.5 [mol kg^{-1} bar^{-1}]).

In total, 192 different optimization processes are performed. For each optimization, the Henry coefficient and dimensionless mass transfer coefficient for both components (CH_4 and CO_2) are fitted to the experimental breakthrough curves. In Fig. 3, the distribution of Henry coefficients obtained for CO_2 in different runs are shown. Different colors represent different fixed values of Péclet number. As shown in Fig. 3, there is a clear distinction between the results obtained for different fixed values of Péclet number. For cases with the low Péclet number (high dispersion coefficient), Henry coefficient of CO_2 is underestimated. This under estimation reduces by increasing the Péclet number. As discussed in the previous section, by reducing the Péclet number the breakthrough time of hydrogen reduces leading to the shift of breakthrough curves to the right. The objective of the optimization algorithm is to minimize the deviation between the theoretical and experimentally measured breakthrough curves by varying the values of mass transfer and Henry coefficients of the two components. Therefore, in the optimization algorithm, the shift to the right due to the under estimation of Péclet number is compensated by the underestimation of the Henry coefficients which shifts the breakthrough curves to the left. The highest value of Péclet number (no dispersion) leads to the most accurate estimation of Henry coefficient of CO_2. An other observation from Fig. 3 is that for each Péclet number, as the value of objective function reduces the estimated Henry coefficients are converging to a certain value. One would expect the lowest absolute difference between the estimated Henry coefficients and those measured experimentally to

occur when the global minimum is found. The data presented in Fig. 3 shows exactly the expected shape. For the case with highest value of Péclet number, the global minimum corresponds to the lowest absolute difference between the estimated Henry coefficients and the experimental ones. Therefore, one can conclude that $Pe = \infty$ is an appropriate value for the Péclet number of the system under study.

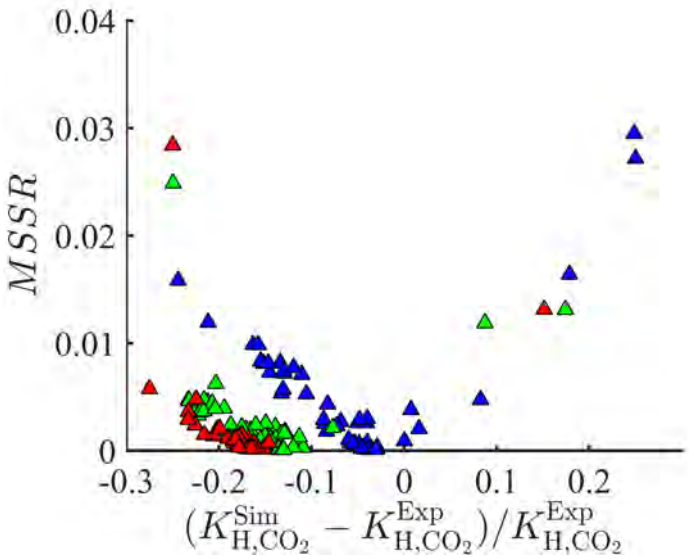

Figure 3: Distribution of values of $MSSR$ as a function of obtained Henry coefficients for CO_2 for different fixed values of Péclet number $Pe = \infty$ (blue), $Pe = 500$ (green) and $Pe = 250$ (red). Fitted Henry coefficients are obtained by fitting the theoretical breakthrough curves to the experimental breakthrough curves. An equimolar mixture of CO_2 and CH_4 is adsorbed by ITQ-29 zeolite at 2 bar and 298 K. The values for Henry coefficients obtained from the experiments are shown in SI

Independent of the value of the mass transfer coefficients, the Henry coefficients predicted by the model are close to the values measured experimentally. This shows even without detailed information regarding the characteristics of a system, one should be able to estimate the Henry coefficients for all components with only rough estimations for the mass transfer coefficients. However, the value of the objective function (quality of the fit) is a function of the estimated mass transfer coefficient. Therefore, better estimations of mass transfer coefficient will result in lower values of objective function and as a consequence better agreement between the theoretical and experimental breakthrough curves. The experimental breakthrough curves and the fitted breakthrough curves for the lowest values of the objective functions are shown Fig. 4. The obtained Henry coefficients are presented in Table 1.

4.3. Estimation of Langmuir isotherms

In this section, the capability of the proposed method for predicting adsorption isotherms beyond the Henry region is investigated. For this purpose experimental breakthrough curves at 11 and 16 bar are used. Experimental conditions, except the pressure of the column, are identical to those of the breakthrough experiments at 2 bar. The experimental adsorption

Table 1: Henry coefficients, mass transfer coefficients and saturation loadings estimated by the mathematical model for low (2 [bar]) and high (11, 16 [bar]) pressure cases ($K^{exp}_{H,CO_2} = 1.2$ [mol kg^{-1} bar^{-1}], $K^{exp}_{H,CH_4} = 0.3$ [mol kg^{-1} bar^{-1}], These values are calculated from independent equilibrium adsorption experiments.)

Component	Pressure [bar]	k'_L	K_H [mol kg^{-1} bar^{-1}]	q_{sat} [mol kg^{-1}]
CO_2	2	4.35 +/- 0.004	1.16 +/- 0.01	-
CH_4	2	1.47 +/- 0.064	0.36 +/- 0.01	-
CO_2	11,16	6.3 +/- 0.36	1.50 +/- 0.13	6.56 +/- 0.01
CH_4	11,16	2.6 +/- 0.15	0.48 +/- 0.08	3.20 +/- 0.004

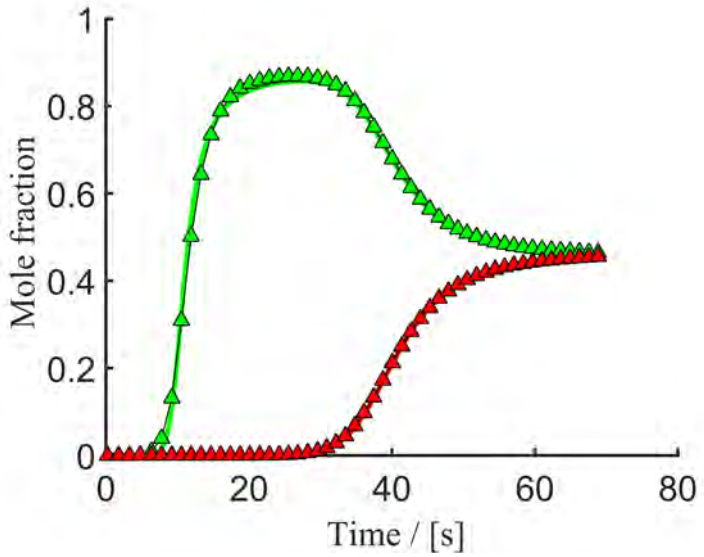

Figure 4: Experimental breakthrough data (symbols) and theoretical breakthrough curves (lines) obtained for the optimized estimated parameter, $Pe = \infty$. An equimolar mixture of CO_2 (red) and CH_4 (green) is adsorbed by ITQ-29 zeolite at 2 bar and 298 K.

isotherms for CO_2 and CH_4 in ITQ-29 at 298 K are described very well by Langmuir functional forms. To facilitate the use of IAST, Langmuir adsorption isotherms are assumed for pure CO_2 and CH_4. It should be notes that any other functional forms (e.g. Freundlich or Langmuir-Freundlich) can also be used depending on the system under study. The procedure for predicting the Langmuir adsorption isotherms is similar to the procedure used for predicting the Henry coefficients. Therefore, in this case, the Henry coefficient, the saturation loading corresponding to the adsorption of CO_2 and CH_4 in ITQ-29, dimensionless mass transfer coefficients of the two components and Péclet number are the possible variables for the fitting process. Assuming no dispersion for high pressure case reduces the number of fitting parameters to 6: Henry coefficients, saturation loadings and dimensionless mass transfer coefficients of the two components. The experimental breakthrough curves and the fitted breakthrough curves for the lowest values of the objective functions $MSSR$=0.0021 are shown Figs. 5a and 5b.

In Fig. 6, the predicted adsorption isotherms corresponding to the lowest value of the

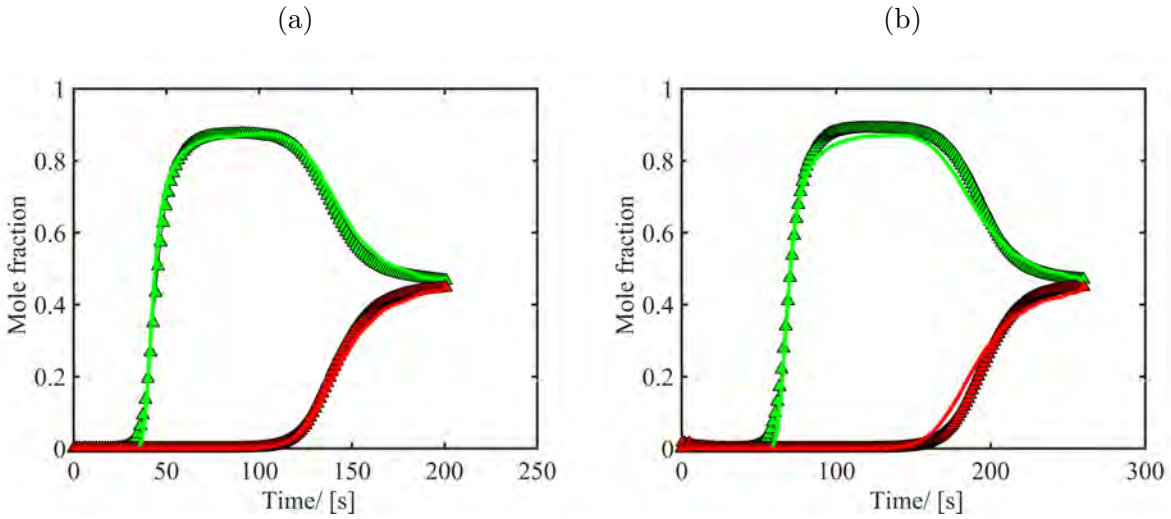

Figure 5: Experimental breakthrough data (symbols) and theoretical breakthrough curves (lines) obtained for the optimized estimated parameter, $Pe = \infty$. An equimolar mixture of CO_2 (red) and CH_4 (green) is adsorbed by ITQ-29 zeolite (a) at 11 bar (b) at 16 bar and 298 K.

objective function among all different simulations are compared with the experimentally measured adsorption isotherms for the adsorption of CO_2 and CH_4 in ITQ-29 at 298 K. The method is well capable of predicting the whole adsorption isotherm for both CO_2 and CH_4 ($MSSR_{CO_2}$=0.16 and $MSSR_{CH_4}$=0.023). As discussed in previous sections, accurate estimation of mass transfer coefficients is not always straightforward. Therefore, it is important to examine the influence of the mass transfer coefficients on the breakthrough curves and corresponding estimated adsorption isotherms. For the case of estimation of Langmuir adsorption isotherms, although mass transfer coefficients are distributed in a wide range, they do not have a noticeable influence on the estimated adsorption isotherms and their agreement with the experimental ones. Therefore, it can be concluded that for the proposed approach a rough estimation of mass transfer coefficients is sufficient. It is not always known whether the conditions of the experiment are within the Henry region or beyond that. Therefore, it is important to investigate the possibility to verify the adequacy of the function form used for the fitting process. In the interest of assessing that, instead of Langmuir adsorption isotherm Henry adsorption isotherm is assumed for the fitting of the theoretical breakthrough curves to the experimental ones at pressures of 11 and 16 bar. It is realized that in this case, the lowest values of the objective functions ($MSSR$=0.023) is an order of magnitude greater than the lowest values of the objective functions ($MSSR$=0.0021) for the case where appropriate functional forms were used for the two components. There are also noticeable differences between the fitted and experimental breakthrough curves. These could indicate that the functional form used for the adsorption isotherms is not appropriate.

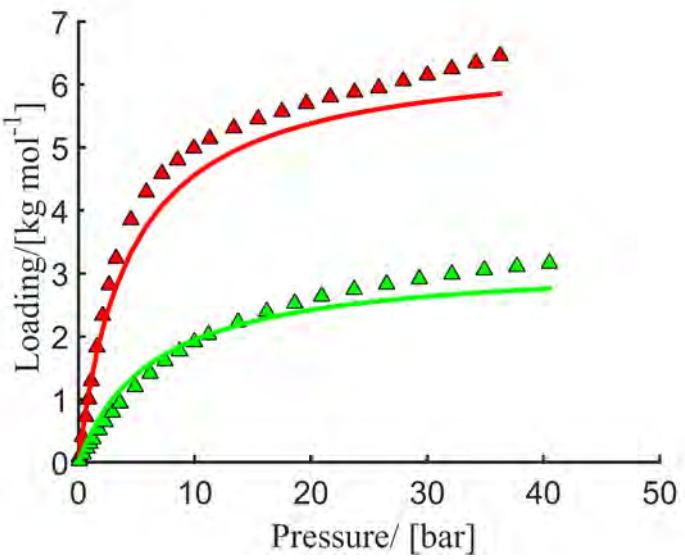

Figure 6: Isotherms based the parameter values estimated from the breakthrough fitting (lines) and experimental data from independently measured isotherms (symbols) adsorption isotherms obtained for the adsorption of pure CO_2 (red) and CH_4 (green) by ITQ-29 zeolite at 298 K. $MSSR_{CO_2}$=0.16 and $MSSR_{CH_4}$=0.023.

5. Conclusion

In this study, we applied a mathematical model describing transient adsorption processes to investigate the effect of the mass transfer rate and dispersion in the gas phase on the shape of breakthrough curves. Higher mass transfer rate between the gas phase and adsorbed phase results in steeper breakthrough curves and longer breakthrough times, while higher dispersion in the gas phase has the opposite effect. The application of an appropriate model is not limited only to prediction of the breakthrough curves. We estimated the Henry coefficients and complete Langmuir adsorption isotherm by minimizing the deviation between the theoretical breakthrough curves (computed by model) and those measured experimentally. The adsorption isotherms obtained from our approach are in excellent agreement with the experimental values. Using our approach, one is capable of estimating the adsorption isotherms even without detailed knowledge regarding the mass transfer characteristics of the system. Rough estimations of the mass transfer and dispersion coefficients are sufficient to reproduce the absolute adsorption isotherm from the breakthrough curves. Our approach has the following advantages over the conventional method of extracting adsorption data from breakthrough experiments by equilibrium theory: (1) integration is always accompanied by a level of uncertainty which can result in deviations between the calculated amount of adsorption and real adsorption. This is eliminated in our approach by the direct use of breakthrough curves; (2) the number of experiments which are required to estimate the adsorption isotherms are significantly reduced in our approach. (3) in contrast to the conventional equilibrium theory, our method is suitable for the cases with significantly eroded breakthrough curves (significant kinetic effects). (4) Our approach is applicable for mixture of gases and one can obtain the single component adsorption isotherms from experiments

performed for a mixture of gases. This is a very important advantage since one can compute the mixture adsorption isotherms at any composition from pure component adsorption isotherms using IAST. Although computational algorithms used in this work are readily extendable to multicomponent mixtures, accurate measurement of multicomponent breakthrough curves might be more complicated. Therefore, future studies are needed to assess the accuracy of the proposed method for multicomponent mixtures

6. Acknowledgements

This work was sponsored by NWO Exacte Wetenschappen (Physical Sciences) for the use of computer facilities, with financial support from the Nederlandse Organisatie voor Wetenschappelijk Onderzoek (Netherlands Organization for Scientific Research, NWO). The authors also gratefully acknowledge the financial support from Shell Global Solutions B.V., and the Netherlands Research Council for Chemical Sciences (NWO/CW) through a VIDI grant (David Dubbeldam) and a VICI grant (Thijs J. H. Vlugt).

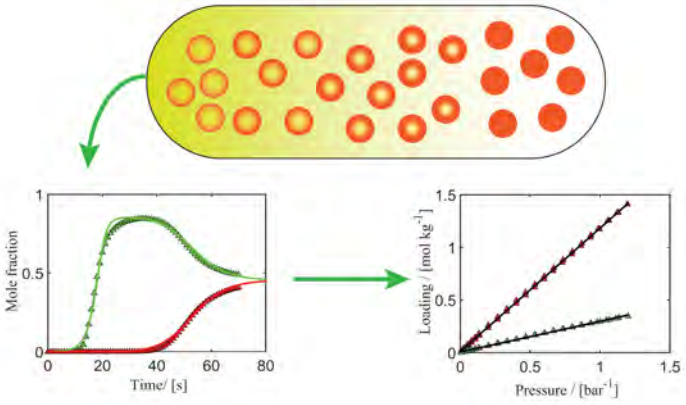

TOC

References

[1] V. G. Gomes, K. W. Yee, Sep. Purif. Technol. 28 (2002) 161 – 171.
[2] H. Yang, Z. Xu, M. Fan, R. Gupta, R. B. Slimane, A. E. Bland, I. Wright, J. Environ. Sci. 20 (2008) 14 – 27.
[3] J. R. Li, R. J. Kuppler, H.-C. Zhou, Chem. Soc. Rev. 38 (2009) 1477–1504.
[4] N. K. Jensen, T. E. Rufford, G. Watson, D. K. Zhang, K. I. Chan, E. F. May, J. Chem. Eng. Data 57 (2012) 106–113.
[5] K. Y. Foo, B. H. Hameed, Chem. Eng. J. 156 (2010) 2 – 10.
[6] P. Serra-Crespo, R. Berger, W. Yang, J. Gascon, F. Kapteijn, Chem. Eng. Sci. 124 (2015) 96 – 108.
[7] M. S. Shafeeyan, W. M. A. W. Daud, A. Shamiri, Chem. Eng. Res. Des. 92 (2014) 961 – 988.
[8] D.-L. Chen, N. Wang, C. Xu, G. Tu, W. Zhu, R. Krishna, Micropor. Mesoporo. Mat. 208 (2015) 55 – 65.
[9] T. Valdés-Solis, M. Linders, F. Kapteijn, G. Marbán, A. Fuertes, Chem. Eng. Sci. 59 (2004) 2791 – 2800.
[10] S. Ghorai, K. Pant, Sep. Purif. Technol. 42 (2005) 265 – 271.
[11] L. H. Shendalman, J. E. Mitchell, Chem. Eng. Sci. 27 (1972) 1449–1458.
[12] J. A. C. Silva, A. Ferreira, P. A. P. Mendes, A. F. Cunha, K. Gleichmann, A. E. Rodrigues, Ind. Eng. Chem. Res. 54 (2015) 6390–6399.
[13] E. D. Bloch, W. L. Queen, R. Krishna, J. M. Zadrozny, C. M. Brown, J. R. Long, Science 335 (2012) 1606–1610.
[14] J. A. Mason, K. Sumida, Z. R. Herm, R. Krishna, J. R. Long, Energy Environ. Sci. 4 (2011) 3030–3040.
[15] W. Zhang, Y. Shan, A. Seidel-Morgenstern, Journal of Chromatography A 1107 (2006) 216–225.
[16] O. Lisec, P. Hugo, A. Seidel-Morgenstern, Journal of Chromatography A 908 (2001) 19–34.
[17] A. Seidel-Morgenstern, Journal of Chromatography A 1037 (2004) 255–272.
[18] R. H. K., A. R., A. N.R., Philosophical Transactions of the Royal Society of London 267 (1970) 419–455.
[19] H. F.G., K. G., Multicomponent Chromatography, Marcel Dekker, New York, 1970.
[20] J. N. Wilson, Journal of the American Chemical Society 62 (1940) 1583–1591.
[21] D. DeVault, Journal of the American Chemical Society 65 (1943) 532–540.
[22] E. Glueckauf, Journal of Chemical Society 10 (1947) 1302–1308.
[23] G. Guiochon, S. Golshan-Shirazi, A. Katti, Fundamentals of nonlinear and preparative chromatography, Academic Press, Boston, 1994.
[24] H.-K. Rhee, R. Aris, N. R. Amundson, First-Order Partial Differential Equations, Volume I, Theory and Application of Single Equations, Prentice Hall Inc, Englewood Cliffs, NJ, 1986.
[25] H.-K. Rhee, R. Aris, N. R. Amundson, First-Order Partial Differential Equations, Volume II, Theory and Application of Single Equations, Prentice Hall Inc, Englewood Cliffs, NJ, 1989.
[26] I. Tiscornia, S. Valencia, A. Corma, C. Tellez, J. Coronas, J. Santamaria, Micropor. Mesoporo. Mat. 110 (2008) 303 – 309.
[27] M. Palomino, A. Corma, F. Rey, S. Valencia, Langmuir 26 (2010) 1910–1917.
[28] A. van Miltenburg, J. Gascon, W. Zhu, F. Kapteijn, J. A. Moulijn, Adsorption 14 (2008) 309–321.
[29] S. Ergun, Chem. Eng. Prog. 48 (1952) 89–94.
[30] J. Gascon, W. Blom, A. van Miltenburg, A. Ferreira, R. Berger, F. Kapteijn, Micropor. Mesoporo. Mat. 115 (2008) 585–593.
[31] E. Glueckauf, Trans. Faraday Soc. 51 (1955) 1540–1551.
[32] D. G. Hartzog, S. Sircar, Adsorption 1 (1995) 133–151.
[33] D. M. Ruthven, Principles of adsorption and adsorption processes, John Wiley & Sons, New York, 1984.
[34] S. Sircar, J. R. Hufton, Adsorption 6 (2000) 137–147.
[35] A. L. Myers, J. M. Prausnitz, AIChE J. 11 (1965) 121–127.
[36] D. W. Hand, S. Loper, M. Ari, J. C. Crittenden, Environ. Sci. Technol. 19 (1985) 1037–1043.
[37] L. Kheifets, D. Predtechenskaya, Russ. J. Phys. Chem. 80 (2006) 196–199.
[38] R. Krishna, J. M. van Baten, Chem. Phys. Lett. 446 (2007) 344 – 349.

[39] R. Krishna, J. M. Van Baten, Sep. Purif. Technol. 61 (2008) 414 – 423.
[40] K. S. Walton, D. S. Sholl, AIChE J. 61 (2015) 2757–2762.
[41] R. T. Yang, Gas separation by adsorption processes, Butterworth, Boston, 1997.
[42] J. A. Moulijn, W. P. M. Van Swaaij, Chem. Eng. Sci. 31 (1976) 845–847.
[43] W. E. Schiesser, The numerical method of lines: integration of partial differential equations, Elsevier Bethlehem Pennsylvania, 2012.
[44] A. Torres-Knoop, R. Krishna, D. Dubbeldam, Angew. Chem. Int. 53 (2014) 7774–7778.
[45] H. Yu, X. Wang, C. Xu, D.-L. Chen, W. Zhu, R. Krishna, Chem. Eng. J. 269 (2015) 135–147.
[46] J. C. Knox, A. D. Ebner, M. D. LeVan, R. F. Coker, J. A. Ritter, Industrial & Engineering Chemistry Research 55 (2016) 4734–4748.
[47] A. Hatzikioseyian, M. Tsezos, F. Mavituna, Hydrometallurgy 59 (2001) 395 – 406.
[48] H. Yoshida, T. Kataoka, D. M. Ruthven, Chem. Eng. Sci. 39 (1984) 1489–1497.
[49] N. S. Raghavan, D. M. Ruthven, AIChE J. 29 (1983) 922–925.
[50] M. Gholami, M. R. Talaie, Ind. Eng. Chem. Res. 49 (2010) 838–846.

Supporting Information for: Prediction of adsorption isotherms from breakthrough curves

Ali Poursaeidesfahani[a], Eduardo Andres-Garcia[b], Martijn de Lange[a], Ariana Torres-Knoop[c], Marcello Rigutto[d], Nitish Nair[e], Freek Kapteijn[b], Jorge Gascon[f], David Dubbeldam[c], Thijs J.H. Vlugt[a,]

[a] *Engineering Thermodynamics, Process & Energy Department, Faculty of Mechanical, Maritime and Materials Engineering, Delft University of Technology, Leeghwaterstraat 39, 2628CB, Delft, The Netherlands*

[b] *Chemical Engineering Department, Catalysis Engineering, Faculty of Applied Sciences, Delft University of Technology, Julianalaan 136, 2628 BL Delft, The Netherlands*

[c] *Van't Hoff Institute for Molecular Sciences, University of Amsterdam, Science Park 904, 1098XH Amsterdam, The Netherlands*

[d] *Shell Global Solutions International, PO Box 38000, 1030BN Amsterdam, The Netherlands*

[e] *Shell India Markets Private Limited, Kundanahalli Main Road, Bangalore 560048, Karnataka, India*

[f] *KAUST Catalysis Center, Advanced Catalytic Materials, Thuwal 23955, Saudi Arabia*

Email address: t.j.h.vlugt@tudelft.nl (Thijs J.H. Vlugt)

Preprint submitted to Microporous and Mesoporous Materials *March 6, 2018*

In this supporting information, we explain the empirical correlations used to estimate the effective mass transfer coefficient (k_L) and the axial dispersion coefficient.

1. Effective mass transfer and axial dispersion coefficients

The meaning of the effective mass transfer coefficient (k_L) depends on the highest resistance to mass transfer in a system. Silva et al. posed an effective LDF mass transfer coefficient including both external mass transfer as well as macropore diffusion [1]:

$$\frac{1}{k_L} = \frac{r_p}{3k_\mathrm{f}} + \frac{r_p^2}{15D_\mathrm{eff}} \tag{1}$$

Here r_p is the characteristic length of adsorbent particles (e.g. mean radius of particles for spherical particles), k_f is the film mass transfer coefficient, and the effective diffusivity D_eff is expressed as:

$$D_\mathrm{eff} = \frac{\varepsilon_p}{\tau_f} D_p \tag{2}$$

where ε_p and τ_f are the porosity of the adsorbent and the tortuosity. The diffusion coefficient (D_p) can be written as a combination of Knudsen (D_K) and molecular diffusivity (D_M)[2, 3, 4]:

$$\frac{1}{D_p} = \frac{1}{D_K} + \frac{1}{D_M} \tag{3}$$

Further, D_K in turn can be written as [5]:

$$D_K = \frac{d_p}{3}\sqrt{\frac{8RT}{\pi M}} \tag{4}$$

where d_p is the nominal pore diameter of adsorbent, M is the molar mass of adsorbate, R is the universal gas constant and T is the temperature. For the estimation of molecular diffusion coefficients, one could e.g. use the group-contribution methods provided by Poling et al. [6]. The value 15, (right-hand side of Eq. 1) was first derived by Glueckauf [7], by comparing theoretical chromatograms of different mass transfer models. The same value (15) has been recommended for process design by Ruthven [8]. Although this value is not appropriate for very short cycle times[9], it is sufficient for breakthrough simulations in this work.

The axial dispersion coefficient can be estimated knowing the Schmidt and Reynolds numbers[10, 11]. Axial dispersion is caused by two spreading mechanisms: (1) molecular diffusion (2) eddy diffusion. In general, the axial dispersion coefficient is a function of Reynolds number and therefore it changes along the column when appreciable amounts are adsorbed. At low Reynolds number, the molecular diffusion is the main spreading mechanism in the axial direction and the effect of eddy diffusion can neglected[12, 13]. The molecular diffusion coefficient is given by[14]:

$$D_{M,g} = \frac{CT^{1.5}\sqrt{\frac{1}{M_1} + \frac{1}{M_2}}}{p\sigma_{12}^2\Omega} \tag{5}$$

where C is a constant, M_i is the molar mass of component i, $\sigma_{ij} = (\sigma_i + \sigma_j)/2$ is the average collision diameter and Ω is the temperature-dependent collision integral.

2. Adsorption isotherm Henry region

The experimentally measured adsorption isotherm of pure CO_2 and CH_4 at 298 K in zeolite ITQ-29 are shown in Fig. 1.

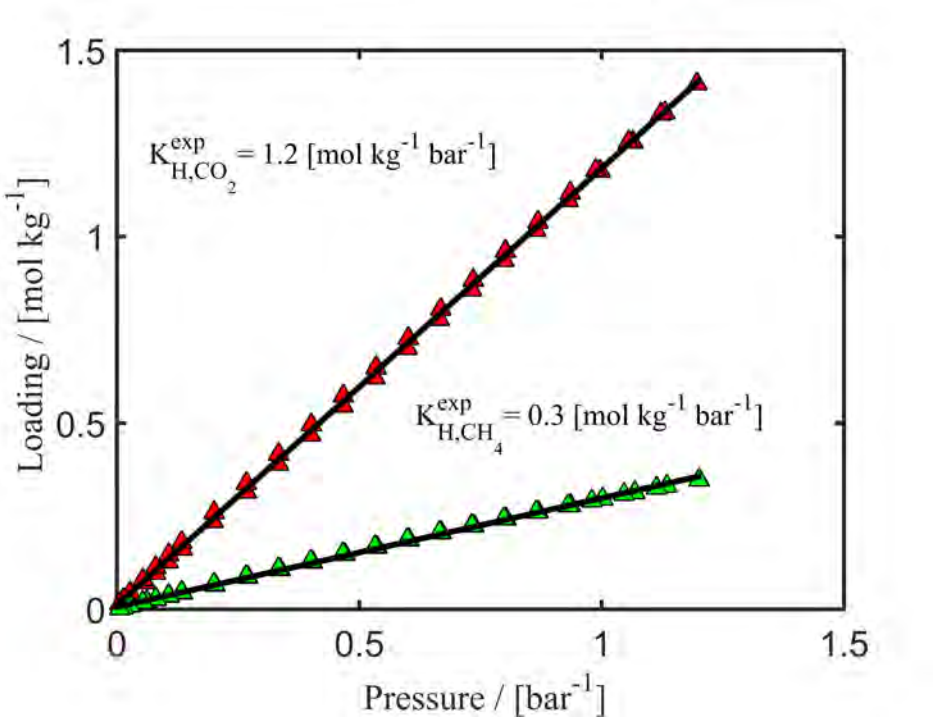

Figure 1: Experimentally measured adsorption isotherm of pure CO_2 and CH_4 at 298 K in zeolite ITQ-29. Symbols show the experimentally measured values. The Henry coefficients are obtained by the slope of the line fitted to the data points (solid lines).

References

[1] J. A. C. Silva, A. Ferreira, P. A. P. Mendes, A. F. Cunha, K. Gleichmann, A. E. Rodrigues, Ind. Eng. Chem. Res. 54 (2015) 6390–6399.

[2] M. S. Shafeeyan, W. M. A. W. Daud, A. Shamiri, Chem. Eng. Res. Des. 92 (2014) 961 – 988.

[3] C. A. Grande, F. V. S. Lopes, A. M. Ribeiro, J. M. Loureiro, A. E. Rodrigues, Sep. Sci. Technol. 43 (2008) 1338–1364.

[4] R. T. Yang, Gas separation by adsorption processes, Butterworth, Boston, 1997.

[5] J. Gilron, A. Soffer, J. Membr. Sci. 209 (2002) 339 – 352.

[6] R. C. Reid, J. M. Prausnitz, B. E. Poling, The properties of gases and liquids, McGraw-Hill, New York, 1987.

[7] E. Glueckauf, Trans. Faraday Soc. 51 (1955) 1540–1551.

[8] D. M. Ruthven, Principles of adsorption and adsorption processes, John Wiley & Sons, New York, 1984.

[9] S. Sircar, J. R. Hufton, Adsorption 6 (2000) 137–147.

[10] O. Levenspiel, Chemical reaction engineering, John Wiley & Sons, New York, 1972.

[11] K. B. Bischoff, Ph.D. Thesis, Chemical Engineering Department, Illinois Institute of Technology, 1961.

[12] J. A. Moulijn, W. P. M. Van Swaaij, Chem. Eng. Sci. 31 (1976) 845–847.

[13] S. T. Sie, G. W. A. Rijnders, Analytica Chimica Acta 38 (1967) 3–16.

[14] J. O. Hirschfelder, C. F. Curtiss, R. B. Bird, M. G. Mayer, Molecular theory of gases and liquids, volume 26, Wiley New York, 1954.